



HAL
open science

An inverse problem of elastostatics in mechanics of composites

A.N. Galybin

► **To cite this version:**

A.N. Galybin. An inverse problem of elastostatics in mechanics of composites. *Composites Science and Technology*, 2009, 68 (5), pp.1188. 10.1016/j.compscitech.2007.05.027 . hal-00524474

HAL Id: hal-00524474

<https://hal.science/hal-00524474>

Submitted on 8 Oct 2010

HAL is a multi-disciplinary open access archive for the deposit and dissemination of scientific research documents, whether they are published or not. The documents may come from teaching and research institutions in France or abroad, or from public or private research centers.

L'archive ouverte pluridisciplinaire **HAL**, est destinée au dépôt et à la diffusion de documents scientifiques de niveau recherche, publiés ou non, émanant des établissements d'enseignement et de recherche français ou étrangers, des laboratoires publics ou privés.

Accepted Manuscript

An inverse problem of elastostatics in mechanics of composites

A.N. Galybin

PII: S0266-3538(07)00229-1
DOI: [10.1016/j.compscitech.2007.05.027](https://doi.org/10.1016/j.compscitech.2007.05.027)
Reference: CSTE 3720

To appear in: *Composites Science and Technology*

Received Date: 8 March 2007
Revised Date: 9 May 2007
Accepted Date: 16 May 2007



Please cite this article as: Galybin, A.N., An inverse problem of elastostatics in mechanics of composites, *Composites Science and Technology* (2007), doi: [10.1016/j.compscitech.2007.05.027](https://doi.org/10.1016/j.compscitech.2007.05.027)

This is a PDF file of an unedited manuscript that has been accepted for publication. As a service to our customers we are providing this early version of the manuscript. The manuscript will undergo copyediting, typesetting, and review of the resulting proof before it is published in its final form. Please note that during the production process errors may be discovered which could affect the content, and all legal disclaimers that apply to the journal pertain.

An inverse problem of elastostatics in mechanics of composites

A.N. Galybin

Wessex Institute of Technology, Southampton, UK

Phone +44 (0) 238 029 3223; E-mail: agalybin@wessex.ac.uk

Abstract

In this study we consider an inverse problem of elastostatics and its applications appearing in mechanics of composites. In many cases surface displacements can be monitored on a part of a stress-free boundary of an elastic composite (in general, heterogeneous). When this information is further used for stress analysis it leads to redundancy in boundary conditions on the part where displacements have been measured. To compensate this redundancy no boundary conditions are imposed on some internal boundaries such as cracks, inclusions or interfaces between dissimilar materials in a particular composite. As the result one arrives to an ill-posed boundary value problem of elasticity overspecified on a part of the entire boundary and underspecified on the rest of it. This paper presents general approach based on integral equations and studies one particular example for the reconstruction of characteristics of narrow process zones developing near the crack tips.

Key words: B. Fracture; B. Interface; C. Crack; C. Delamination; Inverse problems

1. Introduction

Boundary value problems, BVPs, in mechanics of composites often employ the elastic assumption and certain relationships on the interfaces within considered bodies. These relationships usually express continuity of tractions, stresses or displacements across the boundary (or its part) between two (or more) contacting materials having, in general, different elastic properties. Due to the presence of interfaces one needs to consider simultaneously the problem for exterior and interior domains bounded by the same contours. Apart from this, there is no essential differences with the usual BVP of elasticity.

Classical formulation of elastic BVPs requires one of the following surface conditions to

be known on the boundary of a domain: (i) stress vector or tractions; (ii) displacement vector; or (iii) certain combinations of stress and displacement components (mixed problems, widely used in formulations of contact problem). The boundary conditions should be posed on the entire boundary and should not be overspecified, i.e., for instance, stress and displacement vectors should not be given simultaneously on any part of the boundary. Then all the cases (i)-(iii) yield a well-posed BVP with unique and stable solution. The theory of classical BVPs of plane elastostatics is fully presented in the classical monograph by Muskhelishvili [1]. Different types of contact conditions are discussed in detail in Johnson [2], they also lead to well-posed formulations.

However there are many applications where data on stresses or displacements may not be available on the entire boundary of a body (including internal boundaries). Such problems appear in strain-stress measurements, interferometry, rock mechanics, monitoring the fracture development in strength tests etc. They require the consideration of a specific BVP, which is overspecified on a part of the boundary and underspecified on the rest of it. In order to reduce such a problem to one of the conventional types one needs to recover boundary conditions on the entire boundary, therefore they are often referred to as inverse problems. It is known [3] that inverse problem are usually ill-posed in the sense that their solutions are unstable, i.e. small perturbations in boundary conditions lead to essentially different solutions.

Overview of recent results and approaches for solving inverse problems in different fields is presented by Bonnet and Constantinescu [4], in particular, they have mentioned some problems related to mechanics of composites such as identification of distributions of elastic moduli and parameters or buried objects as well as detection of different defects, for instance, cracks. All these problems can be effectively reduced to the inverse problem described above.

During the last two decades there have been numerous attempts to solve problems of this (or close) type in respect to different engineering problems. Earlier works became available in late 80th -mid 90th. Most of them employed methods based on integral equations, see, for

instance, [5] for identification of flaw shape in a body, [6] for overview of inverse problems in fracture mechanics, [7] for contact problems where measurements at the contact area are difficult, [8] for taking into account plastic flow near crack tips, [9] for non-destructive cavity identification, [10] for analytic solutions in half-plane for surface subsidence monitoring, [11,12] for providing integral equations. Finite element formulations have also been employed, e.g. [13]. However no complete analysis of solvability and uniqueness have been performed in early numerical studies. Perhaps, the first comprehensive analysis of solvability of these problems has been reported by Shvab [14] for an isotropic elastic domain with the following boundary conditions: displacement vector is given on a part of the boundary simultaneously with the stress vector; the rest of the boundary has no conditions posed. This problem referred further to as tractions-displacements problem, TDP, can be viewed as consecutive problems for holomorphic vectors, on which the proof of uniqueness can be based, e.g. [15]. Methods using complex variables for investigation of TDP in 2D have also been applied, e.g., [16,17].

One can rarely find analytical solutions of the TDP (with exceptions for simple domains, e.g. for wedge-like domains [16]), therefore the development of stable numerical methods has been the main focus during the last years. The considerable progress has recently been achieved on this topic in UK at University of Leeds by L.Marin, L.Elliott, D.B.Ingham, D.Lesnic and D.N.Hào in the development of regularisation techniques, iterative methods and algorithms for solving inverse BVPs of the TDP or close types [18-24]. In particular it has been shown that the methods based on the Tikhonov regularisation provide stable solutions [18] in elastostatics. Other studies, e.g. , [25], confirm this conclusion, in particular, it has been found [20, 26] that the use of the SVD regularisation presents a valuable computational tool in elastostatics.

In the next sections we present general formulation of the plane elastic TDP for the case of a body composed of two dissimilar materials, derive integral equations for this TDP, consider simple cases relevant to mechanics of composites and present details of SVD regularisation. In order to illustrate the approach we consider a TDP for a crack with narrow process zones

developing near the crack tips. We conduct numerical experiments for recovering stresses and crack opening displacements, COD, in these process zones by utilising synthetic data on COD on the opened part of the crack followed by statistical analysis of the results.

2. Formulation and integral equations of the problem

Formulation of TDP

General solution of plane elastic boundary value problems is given by the Kolosov-Muskhelishvili formulae [1] in terms of two holomorphic functions (complex potentials) $\varphi(z)$ and $\psi(z)$ of complex variable $z=x_1+ix_2$. Let Γ be a closed (or open) contour separating the entire complex plane on exterior Ω^+ and interior Ω^- domains that, in general, have different elastic properties, G^\pm (shear moduli) and ν^\pm (Poisson's ratios).

Boundary values of displacements, $\mathbf{w}=(w_1, w_2)$, tractions $\mathbf{t}=(t_1, t_2)$, and stress vector, $\mathbf{p}=(p_1, p_2)$, can be presented as complex valued functions (of complex variable $\zeta \in \Gamma$) w , t and p respectively via boundary values of complex potentials

$$\begin{aligned} 2G^\pm w^\pm &= 2G^\pm (w_1^\pm + iw_2^\pm) = \kappa^\pm \varphi^\pm - \zeta \bar{\varphi}'^\pm - \bar{\psi}^\pm \\ t^\pm &= t_1^\pm + it_2^\pm = \varphi^\pm + \zeta \bar{\varphi}'^\pm + \bar{\psi}^\pm \\ p^\pm &= p_1^\pm + ip_2^\pm = \frac{\partial}{\partial \zeta} t^\pm = \varphi'^\pm + \bar{\varphi}''^\pm + \frac{\partial \bar{\zeta}}{\partial \zeta} (\zeta \bar{\varphi}''^\pm + \bar{\psi}'^\pm) \end{aligned} \quad (1)$$

Hereafter “ \pm ” denote boundary values obtained by approaching Γ from domains Ω^\pm respectively; piecewise elastic constants κ^\pm are defined as $\kappa^\pm = 3-4\nu^\pm$ to for plane strain and $\kappa^\pm = (3-\nu^\pm)(1+\nu^\pm)^{-1}$ for plane stress; the argument, ζ , of complex valued functions is not shown for compactness.

We consider the following BVP formulated in terms of tractions (stresses) and displacements (tractions-displacements problem, TDP)

$$\begin{aligned} \Gamma_0 : \langle t \rangle &= 0 \quad \text{or} \quad \langle p \rangle = 0; \\ \Gamma_1 : \langle w \rangle &= \omega, \quad t^\pm = \tau \quad \text{or} \quad p^\pm = \rho; \\ \Gamma_2 : \langle w \rangle &= 0; \quad \langle t \rangle = 0 \quad \text{or} \quad \langle p \rangle = 0; \end{aligned} \quad (2)$$

Here $\langle f \rangle$ stand for the jump of a quantity across the contour defined as $\langle f \rangle = f^+ - f^-$; the function

$\omega = \omega(\zeta)$ is known from measurements, therefore it is subjected to experimental errors; Γ_0 , Γ_1 and Γ_2 are non-intersecting portions of Γ , such that $\Gamma = \Gamma_0 \cup \Gamma_1 \cup \Gamma_2$, transition points between the parts

Γ_0 and Γ_2 are, in general, unknown.

Reduction to integral equations

It follows from (2) that $\langle t \rangle = 0$ (and/or $\langle p \rangle = 0$) on the entire boundary and therefore the boundary values of holomorphic functions in (1) are expressed through the jump of displacements and the traction $t = t^+ = t^-$ (or the stress vector $p = p^+ = p^-$). In view of the Cauchy integral formula one can present the potentials as

$$\varphi^\pm(z) = \frac{1}{2\pi i} \int_{\Gamma} \frac{g(\eta) d\eta}{\eta - z}, \quad \psi^\pm(z) = \frac{1}{2\pi i} \int_{\Gamma} \frac{h(\eta) d\eta}{\eta - z}, \quad z \in \Omega^\pm \quad (3)$$

Here for simplicity it is assumed that the potentials vanish at infinity (although general case does not present significant difficulties); the function $h(\eta)$ is expressed via the function $g(\eta)$

$h(\eta) = -\bar{\eta} g'(\eta) - \bar{g}(\eta)$ due to continuity of tractions. Bearing in mind that $2G^\pm w^\pm + t^\pm = (\kappa^\pm + 1)\varphi^\pm$

and $\langle w \rangle = \langle \frac{\kappa+1}{2G} \varphi \rangle - \langle \frac{1}{2G} t \rangle$ one obtains the following relationships by the Sokhotski-Plemelj

formulae [1] applied to the potentials in (3)

$$\alpha g + \beta \mathbf{S}g = \gamma t + \langle w \rangle, \quad \alpha = \frac{\kappa^+ + 1}{4G^+} + \frac{\kappa^- + 1}{4G^-}, \quad \beta = \frac{\kappa^+ + 1}{4G^+} - \frac{\kappa^- + 1}{4G^-}, \quad \gamma = \frac{1}{2G^+} - \frac{1}{2G^-} \quad (4)$$

Operator $\mathbf{S}g$ introduced in (4) has the following properties

$$\mathbf{S}g = \frac{1}{\pi i} \int_{\Gamma} \frac{g(\eta) d\eta}{\eta - \zeta}, \quad \mathbf{S}(\mathbf{S}g) = g, \quad \overline{\mathbf{S}g} = -\mathbf{S}\bar{g} - \mathbf{R}_1 \bar{g}, \quad \mathbf{R}_1 g = \frac{1}{\pi i} \int_{\Gamma} \left(\frac{\eta - \zeta}{\bar{\eta} - \bar{\zeta}} \frac{d\bar{\eta}}{d\eta} - 1 \right) \frac{g(\eta)}{\eta - \zeta} d\eta \quad (5)$$

from which it is also evident that $\mathbf{S}g$ is singular operator while $\mathbf{R}_1 g$ is regular operator.

It should be noted that expressions (3)-(5) preserve their form if boundary conditions employ continuity of the stress vector across the boundary (instead continuity of tractions), in this case the function $g(\eta)$ has to be replaced by its derivative as well as complex potentials.

In the case $\Gamma_0 = \emptyset$ one faces an overspecified problem, which is evident from the fact that the jumps of displacements and tractions determine unique solutions in both domains (see for instance, Savruk [27]).

In the general case $\Gamma_0 \neq \emptyset$ the problem is overspecified on Γ_1 and underspecified on Γ_0 , which allows one to find unique solutions for both domains. They can be derived simultaneously, for which it is sufficient to determine $g(\eta)$ on Γ_0 from an integral equation that is

derived as follows. Firstly let us obtain an expression for tractions, $t=t^+=t^-$ via $g(\eta)$ on Γ that follows from (1) by taking into account equations (3)-(5)

$$t = \mathbf{Q}g, \quad \mathbf{Q}g = \mathbf{S}g - \frac{1}{2}\mathbf{R}_1g - \frac{1}{2}\overline{\mathbf{R}_2g} \quad (6)$$

where \mathbf{I} is the identity operator and regular operator \mathbf{R}_2 has the form

$$\mathbf{R}_2g = \frac{1}{\pi i} \int_{\Gamma} \frac{\bar{\eta} - \bar{\zeta}}{\eta - \zeta} g'(\eta) d\eta = \frac{1}{\pi i} \int_{\Gamma} \left(\frac{\bar{\eta} - \bar{\zeta}}{\eta - \zeta} - \frac{d\bar{\eta}}{d\eta} \right) \frac{g(\eta)}{\eta - \zeta} d\eta \quad (7)$$

Substitution of (6) into (4) results in the following relationships between COD and auxiliary function $g(\eta)$

$$\langle w \rangle = \mathbf{T}g, \quad \mathbf{T}g = \alpha g + \delta \mathbf{S}g + \gamma \mathbf{R}_1g + \gamma \overline{\mathbf{R}_2g}, \quad \delta = \frac{\kappa^+ - 1}{4G^+} - \frac{\kappa^- - 1}{4G^-} \quad (8)$$

Now one can derive integral equations of BVP specified by (2) in one of the following equivalent forms

$$\mathbf{TQ}^{-1}t = \omega \quad \text{on } \Gamma_1 \quad \text{or} \quad \mathbf{QT}^{-1}\langle w \rangle = \tau \quad \text{on } \Gamma_1 \quad (9)$$

To invert operator \mathbf{Q} one should solve the integral equation of the first boundary value problem of plane elasticity presented by (6). It has a unique and stable solution, which is symbolically denoted here as the inverse operator \mathbf{Q}^{-1} . Despite \mathbf{Q}^{-1} is stable, equation (9) belongs to the class of ill-posed problems [3], because it is a Fredholm-type equation of the first kind. The latter is evident if one exchanges the order of operators in (9); it can be shown that although $\mathbf{SQ}^{-1}t$ produces non-integral term βt known on the boundary Γ_1 and all other (integral) terms are written on $\Gamma_0 \cap \Gamma_2$. Therefore operator \mathbf{S} is not singular and (9) is a Fredholm equation of the first kind. Similar conclusion is valid for $\mathbf{T}^{-1}\mathbf{Q}$.

Special cases

In special cases of geometry equations (9) can be radically simplified. Two cases presented in this subsection are of particular interest in mechanics of composites. They address situations where delamination occurs on the interfaces between two lengthy laminates (the case of half-planes) or between matrix and aggregate (circular inclusion embedded in the plane).

In the case of half planes it is evident that $\mathbf{R}_1 = \mathbf{R}_2 = 0$, therefore $\mathbf{Q}^{-1} = \mathbf{S}$ and the first equation in (9) reads as $\alpha \mathbf{S}t = \omega$ on Γ_1 , which can also be written down in the integral form

$$\frac{\alpha}{\pi i} \left(\int_{-\infty}^a + \int_b^{\infty} \right) \frac{t(\eta)}{\eta - x} d\eta = \omega(x), \quad a < x < b \quad (10)$$

It should be noted that (10) can also be used for the case of a finite rectilinear crack (or even for a number of cracks on the x -axis). However more accurate numerical results will be obtained if instead of infinity in (10) one uses actual coordinates of the crack ends. Then the operator \mathbf{Q}^{-1} will have correct behaviour near the ends and the continuity condition on the rest of the x -axis is automatically satisfied. The next section investigates a finite crack in detail.

In the case of unit circular inclusion embedded in the plane $\zeta = e^{i\vartheta}$, $-\pi < \vartheta \leq \pi$ hence

$\bar{\zeta} = \zeta^{-1}$ and regular operators become

$$\mathbf{R}_1 g = \frac{-1}{\pi i} \int_{\Gamma} \frac{g(\eta)}{\eta} d\eta = -2\varphi(0) = 0, \quad \mathbf{R}_2 g = -\frac{2c}{\zeta}, \quad c = \frac{1}{2\pi i} \int_{\Gamma} \frac{g(\eta)}{\eta^2} d\eta = \varphi'(0), \quad \text{Im } c = 0 \quad (11)$$

The inverse operator assumes the form $g(\eta) = \mathbf{S}t - c\eta$, therefore (9) can be transferred into the following integral form

$$\frac{\alpha}{\pi} \left(\int_{-\pi}^{\vartheta_1} + \int_{\vartheta_2}^{\pi} \right) \frac{e^{i\theta} t(\theta)}{e^{i\theta} - e^{i\vartheta}} d\theta = \omega(\vartheta) + c(\alpha + \beta)e^{i\vartheta}, \quad \vartheta_1 < \vartheta < \vartheta_2 \quad (12)$$

After integration of the inverse operator ($g(\eta) = \mathbf{S}t - c\eta$) divided by η^2 one finds an expression for the unknown constant c through the tractions in the form

$$c = \frac{1}{4\pi i} \int_{\Gamma} \frac{t(\zeta)}{\zeta^2} d\zeta = \frac{1}{4\pi} \left(\int_{-\pi}^{\vartheta_1} + \int_{\vartheta_2}^{\pi} \right) e^{-i\theta} t(\theta) d\theta \quad (13)$$

It is evident that c is real because the imaginary part of the integral vanishes due to global equilibrium (resultant moment and resultant force are both zero). Now the constant c is found from the linear system obtained after solving (12) followed by the substitution of the solution for $t(\theta)$ into (13).

Numerical solution

Due to ill-posedness any solution of (9) is unstable and special regularisation is required to obtain stable approximate solutions. Here we use the SVD regularisation that, as shown in [20,26], is an effective tool for this type of problems.

First of all equations (8) or (9) are reduced to a linear system of algebraic equation $\mathbf{AC}=\mathbf{W}$. This system can be obtained by different methods. In this study, we seek solutions as linear combinations of independent functions, $f_j(\eta)$ with unknown coefficients $\{c_j\}$, $j=1 \dots n$, which immediately reduces integral equation (9) to a functional equation of the form $c_0F_0(\zeta)+c_1F_1(\zeta)+ \dots+c_nF_n(\zeta)=\omega(\zeta)$ where $F_j(\zeta)$ are functions obtained by applying the operator(s) in the left hand sides of (8) or (9) to $f_j(\eta)$. This functional equation is further converted into the linear system by application of the collocation method with m collocation points, ζ_m , such that array $\{\omega(\zeta_m)\}$ forms the right hand side of the linear system, \mathbf{W} , and $\{F_j(\zeta_m)\}$ its matrix \mathbf{A} . The latter obviously has m rows (equations) and n columns (unknowns), in general, $n \leq m$. Then an approximate solution of this system is found by the SVD method as follows

$$\mathbf{C} = \mathbf{V}^T \mathbf{D}' \mathbf{U} \mathbf{W} \quad (14)$$

Here \mathbf{U} ($m \times n$) and \mathbf{V} ($n \times n$) are orthogonal matrices in the SDV decomposition $\mathbf{A}=\mathbf{U}\mathbf{D}\mathbf{V}^T$ and \mathbf{D} ($n \times n$) is a diagonal matrix formed by the singular values, d_j , placed in descending order on the main diagonal, $d_1 \geq d_2 \geq \dots \geq d_n$; the matrix \mathbf{D}' is the regularised inverse of \mathbf{D} with the rank k : $\mathbf{D}' = \text{diag}\{d_1^{-1}, d_2^{-1}, \dots, d_k^{-1}, 0 \dots 0\}$.

Stability of the solution is controlled by the condition number determined as the ratio of d_1/d_k . In all examples considered further on the condition number is kept below 10^3 .

3. Recovering characteristics of process zones near rectilinear crack

Crack with narrow process zones

The knowledge of stress distribution in an narrow process (cohesive) zone developing on the continuation of the crack ahead of crack tips is fundamental for the investigation of fracture propagation in many quasi-brittle materials such as concretes, rocks, ceramics, alloys, etc. Since 1959 when the first model of process zone for brittle fracture was introduced in [28], a number of theoretical models of the process zone have been suggested, however none of them can be considered as a universal model. Comprehensive survey of up-to-date achievements in this field

can be found in *Engineering Fracture Mechanics* **69** (2) (2002).

A possible general approach can employ experimental data on displacements spread over a sample with the crack followed by the inverse analysis. This procedure is based on solving a system of certain functional equations with respect to parameters describing a softening law in the process zone, [29]. Such a problem belongs to a wide class of identification problems that are usually ill-posed. Paper [30] refers the identification problem to the class of constrained optimisation problems and states that one could face significant difficulties while solving the problem of this type. On the other hand it is possible to treat this problem as a direct one by reducing it to a TDP formulated above. This reduction retains the ill-posed nature of the problem but allows for a relatively simple numerical analysis as compared to the case of the optimisation problem with multiple constrains. The present subsection investigates a general method for the determination of stress distributions inside the process zone proposed in [25,26]. The method uses data on crack opening displacements, COD, as input information.

Integral equation for a straight crack in a plane is obtained from the equation for half-planes differentiated with respect to the contour variable. It is also worth to introduce the crack ends (their positions are in general, unknown) and obvious corrections addressing loads at infinity or on a part of the crack surfaces. In order to illustrate the approach proposed in the previous section let us consider two simple symmetrical cases depicted in Fig 1: cracks subjected to normal loads only, they occupy interval $(-L,L)$ with the traction-free part $(-1,1)$ on which COD are monitored. Integral equation for these cases assumes the following form

$$\frac{-2x}{\pi\sqrt{L^2-x^2}} \int_1^L \frac{\sqrt{L^2-\eta^2} p(\eta)}{\eta^2-x^2} d\eta = \mu(x) - \mu_0(x), \quad 0 \leq x < 1 \quad (15)$$

Here the right hand side is considered as the sum of two terms: the first one is proportional to the derivatives of measured COD, $\mu(x) = \alpha^{-1} \omega'(x)$, while the second one is proportional to COD due to exactly known stresses applied on the crack surfaces and/or at infinity, $\mu_0(x)$. The condition of single-valuedness should be automatically satisfied, which provides uniqueness of the solution of

integral equation (15).

For the determination of unknown crack length (parameter L) it is assumed that the presence of process zones make stresses to be bounded at the crack tips. Therefore the mode I stress intensity factor, K_I , should vanish, which leads to the following condition

$$K_I^0(L) + \frac{2\sqrt{L}}{\sqrt{\pi}} \int_1^L \frac{p(x)}{\sqrt{L^2 - x^2}} dx = 0 \quad (16)$$

where $K_I^0(L)$ corresponds to exactly known stresses and the stress p is solution of (15).

Two cases of loads are considered: uniform tension, σ_0 , at infinity (Fig 1a) and concentrated force, P_0 , applied at the crack centre (Fig 1b). For these cases

$$\mu_0(t) = \frac{1}{\pi\sqrt{L^2 - t^2}} \begin{cases} \pi\sigma_0 t & \text{for uniform load} \\ P_0 L t^{-1} & \text{for concentrated forces} \end{cases} \quad |t| < L \quad (17)$$

$$K_I^0(L) = \begin{cases} \sigma_0 \sqrt{\pi L} & \text{for uniform load} \\ \frac{P_0}{\sqrt{\pi L}} & \text{for concentrated forces} \end{cases} \quad (18)$$

In order to model unknown stresses in the process zone we examine polynomial distributions as described in the next subsection.

Model examples of stress recovering in the process zone

This subsection describes the algorithm used in numerical modelling of the cohesive stress recovering and presents the results of numerical experiments. Modelling undergoes the following major steps.

- ideal distributions of normal stresses acting in the process zone are introduced and ideal densities of COD are calculated;
- synthetic data are generated by adding normally distributed errors to ideal densities of COD;
- stress distributions in the process zone are recovered for different lengths of process zones by solving integral equations (15) followed by recovering the length of the process zone by satisfying the condition of boundedness of the solution (16);
- statistical analysis for different sets of errors has been performed to find out accuracy in the reconstruction.

Synthetic data

The following polynomial distributions of compressive stresses (referred to as ideal stresses further) have been used in modelling

$$p_{ideal}^{(j)} = -(x-1)^j (L_0-1)^{-1}, \quad j = 0 \dots n \quad (19)$$

where j is associated with the numerical test number and L_0 is a given length of the process

zone. It should be noted that different smooth distributions of cohesive stresses can be composed from (19) by means of power series. All distributions (19) are monotonic, vanish at $x=1$ and have minimum magnitude of -1 at the crack tips.

Distributions (19) may occur in the process zones if and only if the applied load is of certain magnitude determined from the condition $K_I=0$. This leads to the following tensile load at infinity

$$\sigma_0^{(j)} = -2(L_0-1)^{-j} J_j(L_0, L_0, 1), \quad j = 0 \dots n \quad (20)$$

or to

$$P_0^{(j)} = -2\pi L_0 (L_0-1)^{-j} J_j(L_0, L_0, 1), \quad j = 0 \dots n \quad (21)$$

for the case of concentrated forces. Hereafter the following integral is used

$$J_k(t, L, a) = \frac{1}{\pi} \int_1^L \frac{\sqrt{L^2 - x^2} (x-a)^k}{x^2 - t^2} dx \quad (22)$$

Dimensionless magnitudes the loads in (20) and (21) are given in Table 1.

Densities of COD corresponding to the distributions presented by formulas (19)-(21) are

$$\mu_\sigma(t) = \frac{t}{\sqrt{L_0^2 - t^2}} \left[\sigma_0^{(j)} + 2(L_0-1)^{-j} J_j(t, L_0, 1) \right], \quad 0 \leq t < L_0 \quad (23)$$

for the case of a uniform load and

$$\mu_P(t) = \frac{1}{\pi t \sqrt{L_0^2 - t^2}} \left[L_0 P_0^{(j)} + 2\pi (L_0-1)^{-j} t^2 J_j(t, L_0, 1) \right], \quad 0 \leq t < L_0 \quad (24)$$

for the case of concentrated forces. They are referred to as ideal densities further on.

Experimental measurements of COD on the visual part of the crack $(-1, 1)$ are obviously subjected to errors. These errors appear only in the right-hand sides of integral equation and linear algebraic system. They are modelled by introducing a distortion in the right hand side of

the linear system. Such a distortion has independently been generated at every collocation point by introducing random errors normally distributed within the range of $\pm 5\%$ of calculated values by formulas (23) or (24). Therefore in the calculations the vector \mathbf{W} had the following components

$$\begin{aligned}\omega_m^\sigma &= (1 + \xi_m) \mu_\sigma(t_m), & \text{for uniform load} \\ \omega_m^P &= (1 + \xi_m) t_m^2 \mu_P(t_m), & \text{for concentrated forces}\end{aligned}\quad (25)$$

where ξ_m ($m=1 \dots M$) are Gaussian errors. In all calculations below the collocation points have been chosen equidistant on $(0, 1)$, i.e. as $t_m = (2m-1)/2M$, $m=1 \dots M$.

Solution

Solution of integral equation (15) is sought in the form

$$p(x) = \sum_{k=0}^n c_k (x-1)^k, \quad 1 \leq x \leq L \quad (26)$$

After substitution of (26) into (15) and (16) one obtains the following functional equations

$$\frac{-2t}{\sqrt{L^2 - t^2}} \sum_{k=0}^n J_k(t, L, 1) c_k = \mu(t) - \mu_0(t), \quad 1 \leq t < L \quad (25)$$

$$K_I^0(L) - 2\sqrt{\pi L} \sum_{k=0}^n c_k J_k(L, L, 1) = 0 \quad (26)$$

It follows from (18) and (26) that the unknown coefficients are linked with the applied loads as

$$\sigma_0 = 2 \sum_{k=0}^n c_k J_k(L, L, 1), \quad P_0 = 2\pi L \sum_{k=0}^n c_k J_k(L, L, 1) \quad (27)$$

Substitution of (27) into (25) with the account for (17) leads to transformed functional equations for the determination of the unknown constants c_k . For the case of uniform loads

$$\frac{2t}{\sqrt{L^2 - t^2}} \sum_{k=0}^n [J_k(L, L, 1) - J_k(t, L, 1)] c_k = \mu(t), \quad 1 \leq t < L \quad (28)$$

For the case of concentrated forces

$$\frac{2t}{\sqrt{L^2 - t^2}} \sum_{k=0}^n [L^2 J_k(L, L, 1) - t^2 J_k(t, L, 1)] c_k = t^2 \mu(t), \quad 1 \leq t < L \quad (29)$$

Accordingly the coefficients $a_{k,j}$ of matrix $\mathbf{A} = \{a_{k,m}\}$ in the linear system are as follows

$$a_{k,m}(L) = \frac{2t_m [J_k(L, L, 1) - J_k(t_m, L, 1)]}{\sqrt{L^2 - t_m^2}}, \quad 0 < t_m < 1, \quad m = 1 \dots M \quad (30)$$

$$a_{k,m}(L) = \frac{2t_m [J_k(L, L, 1) - J_k(t_m, L, 1)]}{\sqrt{L^2 - t_m^2}}, \quad 0 < t_m < 1, \quad m = 1 \dots M \quad (31)$$

The right hand sides of the linear system $\mathbf{AC}=\mathbf{W}$ are given by (25) $\mathbf{W}=\{\omega_m\}$. Its stable solution, vector $\mathbf{C}=\{c_k\}$, is obtained by formula (14), it is evident that this solution depends on L . The latter is further found from (26) as detailed in the next subsection.

The approach employed here has no restriction for studying more complex (although smooth) distributions of stresses in the process zone. General case can be easily obtained if instead of basic distributions (19) their linear combinations are considered. In this case one arrives to polynomial distributions with respect to the powers of $(x-1)$. This does not complicate the analysis since the sought solutions have exactly the same form given by (26).

Numerical results

The normalised length of the process zones, $l=L-1$, has been varied from 0 to 2 in all numerical calculations. The choice of the value for the upper bound is justified by the previous results [25] that have shown satisfactory recovering of the cohesive stresses within this range for the case when the length of the process zone is known (longer process zones are unlikely to be observed in quasi-brittle materials as well). Once solutions c_k depending on the length of the process zone have been obtained, the values of applied loads can be calculated by formulas (27) (for uniform load or for concentrated forces). Then the length of the process zone is recovered by solving the following equations with respect to parameter L

$$\sum_{k=0}^n c_k J_k(L, L, 1) = (L_0 - 1)^{-j} J_j(L_0, L_0, 1) \begin{cases} 1 & \text{uniform load} \\ L_0/L & \text{concentrated force} \end{cases}, \quad j = 0 \dots n \quad (32)$$

Here the coefficients c_k depend on the crack length, L , and the test number, j . The right hand sides in (32) represent the applied loads (Table 1) and solutions are sought within the interval (1,3) for all given L_0 from the same interval. Step-by-step method with correction is used for calculations of the roots, at each step the coefficients c_k have been determined as described above. Due to 10% errors introduced in the right hand side, the accuracy in calculations of the roots has been restricted by 0.01.

Beforehand the problem has been solved for the case when the right-hand sides (25) are known exactly. This has been done in order to determine the number of collocation points in the modelling and to check whether or not the choice of the condition number, C , within 10^2 - 10^3 provides sufficient accuracy in the reconstruction of cohesive stresses. All calculations have been restricted by the fourth order polynomials ($n=4$). It has been found that 2-3 nonzero diagonal elements (of maximum 5) in the matrix \mathbf{D}' provide $C=10^2$ - 10^3 and no significant refinement of results have been observed if M varies from 20 to 100. The number of collocations has been set $M=100$ in all subsequent numerical experiments. The condition number has been set less than 10^3 for the case of uniform load and less than 10^2 for the case of concentrated forces. This choice is explained by much more sensitive behaviour of solutions in regard to distortions imposed in the right hand side in the latter case.

Figure 2 illustrates the recovered and ideal stress distributions in the process zone for the case $j=1$ under uniform loading at infinity for different condition numbers. Digits in the figure refer to the numbers of non-zero terms in the truncated matrix \mathbf{D}' . Corresponding condition numbers are: 1 – $C=1$; 2 – $C\approx 10$; 3 – $C\approx 250$; 4 – $C\approx 8\cdot 10^3$; 5 – $C\approx 4\cdot 10^5$. Figure 2a presents the case when no errors have been imposed in the right hand side of the integral equation. For this case three non-zero elements in \mathbf{D}' give satisfactory accuracy while for four non-zero elements the solution recovered completely coincides with the ideal distribution. Figure 2b presents similar case with 10% errors ($-0.053\leq\xi_m\leq 0.05$) introduced in the right hand side of linear equation. As obvious from the figure curves 4 and 5 deviates from the ideal distribution significantly, these solutions corresponding to $C\approx 8\cdot 10^3$ and $C\approx 4\cdot 10^5$ are unstable. Despite other curves 1-3 are much closer to the ideal distribution, the curves 1-2 show greater errors for the case of the non-disturbed right hand side (Figure 2a). Therefore, 3 non-zero terms are kept in the truncated matrix, which seems to be the best compromise between the accuracy and stability. It is used further on for statistical analysis of the results of numerical experiments.

Statistics

Numerical experiments have been performed in order to estimate the accuracy of reconstruction in the range of the process zone lengths being 0÷2 of the length of the visual part of the crack. For this purpose 200 sets of errors have been generated in the right hand sides for the both types of loading for every case of the ideal stress distributions in the process zone. Polynomial distributions of up to the fourth order have been tested. Then the results obtained have been compared with the ideal solutions obtained for the following set of 14 given lengths: $L_0 = 1.1, 1.25, 1.4, 1.5, 1.6, 1.75, 1.9, 2, 2.1, 2.25, 2.4, 2.5, 2.6, 2.75$.

Two scalar parameters have been calculated in each test. The first one is the ratio

$$\lambda_{jk} = L_{jk} / L_0, \quad j = 0 \dots 4, \quad k = 1 \dots 200 \quad (33)$$

which characterises relative errors in the determination of the length of the process zone. Here L_{jk} are roots of (32) in j^{th} test for k^{th} set of errors. Components λ_{jk} form array Λ which statistical properties are presented in Figure 3.

The second set of parameters computed is the deviations of the recovered stresses from the ideal cohesive stresses, δ_{jk} . These have been calculated by using the L_2 -norm as follows

$$\delta_{ik}^2 = \frac{1}{\min(l_{jk}, l_0)} \int_1^{\min(L_{jk}, L_0)} (p_{jk}(x) - p_{ideal}^{(j)}(x))^2 dx, \quad j = 0 \dots 4, \quad k = 1 \dots 200 \quad (34)$$

Here $l_{jk} = L_{jk} - 1$ are recovered lengths of the process zones; $l_0 = L_0 - 1$ are ideal lengths of the process zones; $p_{jk}(x)$ are recovered distributions of normal stresses in the process zones, $p_{ideal}^{(j)}(x)$ are ideal stresses in the process zones specified by formula (19). The array of deviations δ_{jk} is denoted as Δ further on.

Means and standard deviations of both arrays Λ and Δ have been studied. They are presented in Figures 3-4 as dependencies from ideal lengths of the process zone, l_0 . The results have been obtained for 14 values of parameter L_0 specified above but for the sake of representation all curves have been drawn with the use of cubic spline interpolation.

It is seen from Figure 3 that the poorest case in reconstruction of the process zone length

is the case of uniform distribution of cohesive stresses load ahead of the crack in a plane loaded by uniform load at infinity. In this case the recovered lengths of the process zone deviate more than 15% from the ideal lengths for $l_0 > 1.2$ while standard deviations exceed 0.1. Other types of cohesive loads are reconstructed with higher accuracy of about 10% that corresponds to the level of generated errors. Standard deviations have also tendency to increase as far as length of the process zone increases. This indicates that recovered lengths would have less accuracy being determined for extensive process zones. Figure 6 also indicates that the case $k=0$ for uniform load is a poorest one although the difference with other cases is less pronounced than for array Λ . This agrees with the previous result obtained in [25] with the use of Tikhonov's regularisation method for the case when the length of the process zone is known exactly. The cases $k=0, 1$ seem to be weak among the others for concentrated forces: for $k=1$ the mean is highest when $l_0 > 1$ and the case $k=0$ has highest standard deviations in the range examined. However the difference cannot be referred to as significant.

Both Figures 3 and 4 demonstrate that recovering of process zone characteristics can be performed with satisfactory accuracy within the range $0 < l_0 < 2$. Largest ranges have not been investigated since they can rarely be observed in practice.

Few numerical experiments have been performed in order to investigate how well process zone characteristics can be recovered if the number of terms in (26) is relatively large. In these calculations $n=15$, i.e. the distribution of cohesive stresses has been approximated by polynomials of the 15th order. In particular Figure 5 represents an example of such reconstruction, in which ideal stress was given as power function of the 10th degree ($j=10$ in (19)). The errors have been distributed normally within the range $-0.045 \leq \xi_m \leq 0.039$. As evident from the figure the results of reconstruction are rather good. Statistical analysis in this case has not been performed due to time consuming algorithms used in previous calculations.

Reconstruction of softening laws

The approach can also be used for studying non-linear softening laws in the process zone

of the crack. Typical dependencies used by different researches usually include exponential, power, power-exponential and bilinear (or 3-brach) decaying laws (e.g., [31]). For instance, process zones in concretes may be satisfactory described by bilinear laws in which case three independent parameters are to be determined. It is commonly believed that identification of more than three parameters are unlikely to be done with satisfactory accuracy due to few factors among which are experimental errors and ill-posed nature of the mathematical problem, Bazant [31]. However, an example presented below demonstrates that the accuracy in revealing the softening law by monitoring of the COD is rather satisfactory. This indicates that much greater number of parameters (than 3) describing the softening law can also be recovered. More examples of softening curve recovering can be found in [26].

Let the plane with the crack be loaded uniformly at infinity and the distribution of stresses in the process zone of the length $l_0=1$ be cubic, i.e. $j=3$ and $L_0=2$ in (19) and other formulas used for calculations. The ideal density of crack opening displacements has the form presented in (28) with $\sigma_0^j=0.324$ in this case. Then applying the approach discussed above one determines length, L , distribution of cohesive stresses, p_{rec} , and density of crack opening displacements, μ_{rec} . Both the ideal and recovered crack opening displacements are found by integration as follows

$$g_{ideal}(x) = \int_x^{L_0} \mu_{\sigma}(t) dt, \quad 0 \leq x < L_0, \quad g_{rec}(x) = \int_x^L \mu_{rec}(t) dt, \quad 0 \leq x < L \quad (35)$$

By plotting dependencies of stresses versus crack opening displacements $p_{ideal}=p(g_{ideal})$ and $p_{rec}=p(g_{rec})$ one obtains two softening laws illustrated in Figure 6.

It can be seen from the figure that the difference between the ideal and recovered softening laws is insignificant despite of 10%-errors introduced to model experimental measurements (in this particular case the range is $-0.053 \leq \xi_m \leq 0.05$).

4. Conclusions

This paper presents integral equations for the inverse BVP in mechanics of composites presented by equation (2) in which relative displacements of delaminating surfaces are measured experimentally. Approximate stable solutions of this problem are found by the SDV regularisation of the corresponding linear system of algebraic equations.

Numerical experiments have been performed for a special case in which COD are measured on a part of a crack with narrow cohesive zones. Statistical analysis has shown that the crack length (cohesive zone length) and cohesive stresses can reliably be determined with sufficient accuracy (comparable with the accuracy of COD data) as well as softening laws.

References

1. Muskhelishvili, N.I., Some basic problems of the mathematical theory of elasticity. The Netherlands: P. Noordhoff, Groningen, 1953.
2. Johnson, K.L., Contact mechanics, Cambridge: Cambridge University Press, 1985.
3. Tikhonov, A.N. and Arsenin, V.Y. Solution of Ill-Posed Problems. New York: Winston, Wiley, 1977.
4. Bonnet, M. and A. Constantinescu.. Inverse problems in elasticity. *Inverse Problems*, 2005; 21: R1–R50
5. Tanaka, M. and Y. Masuda . Boundary element method applied to some inverse problems. *Engineering Analysis*, 1986; 3 (3): 138-143.
6. Kubo, S.. Inverse problems related to the mechanics and fracture of solids and structures. *JSME Int. Journal*, 1988; 31: 157-166.
7. Zabararas, N., V. Morellas and D. Schnur. Spatially regularized solution of inverse elasticity problems using the BEM. *Comm. Appl. Numer. Meth.*, 1989; 5: 547-553.
8. Gao, Z. and T. Mura.. Elasticity problems with partially overspecified boundary conditions. *Int Journal of Engineering Science*, 1991; 29 (6): 685-692.
9. Hsieh, S.C. and T. Mura.. Nondestructive cavity identification in structures. *J. Solids Structures*, 1993; 30 (12): 1579-1587.
10. Galybin, A.N.. Solution of a non-classical (inverse) problem for elastic half-plane. In: *Mathematical Modelling in Geological Processes*. Moscow, VNIIGeosystem, 1993. p.131-142.
11. Yeih, W.C., T. Koya and T. Mura. An inverse problem in elasticity with partially overspecified boundary conditions. I. Theoretical approach. *Trans. ASME J. Appl. Mech*, 1993; 60: 595-600.
12. Bui, H. D. Inverse problems in the mechanics of materials: an introduction. Boca Raton, FL: CRC Press. 1994.
13. Schnur, D. and N. Zabararas. Finite element solution of two-dimensional elastic problems using spatial smoothing. *Int. J. Numer. Meth. Engng.*, 1990; 30: 57-75.
14. Shvab, A.A.. Incorrectly posed static problems of elasticity, *Mechanics of Solids*, 1989; 24 (6): 98-106.
15. Schwab, A. A. The inverse problem of elasticity theory: Application of the boundary integral equation for the holomorphic vector. *Phys Solid Earth*, 1994; 30 (4): 342-348.
16. Galybin, A.N., A non-classical plane elastic boundary value problem. In: *Moving*

- Boundaries V WIT Press, Southampton, UK, 1999. p. 59-68.
17. Tselodub, I. Yu.. An inverse problem for an elastic medium containing a physically non-linear inclusion. *J. Appl. Maths Mechs.*, 2000; 64 (3): 407-412.
 18. Marin, L., L. Elliott, D.B. Ingham and D. Lesnic. Boundary element method for the Cauchy problem in linear elasticity, *Eng Analysis with Boundary Elements*, 2001; 25 (9): 783-793.
 19. Marin, L., D.N. Hào and D. Lesnic. Conjugate gradient-boundary element method for the Cauchy problem in elasticity. *Quarterly Journal of Mechanics and Applied Mathematics*. 2002; 55 (2),: 227-247.
 20. Marin, L. and D. Lesnic.. Boundary element solution for the Cauchy problem in linear elasticity using singular value decomposition. *Computer Methods in Applied Mechanics and Engineering*. 2002; 191 (6),3257-3270.
 21. Marin, L., L. Elliott, D.B. Ingham and D. Lesnic.. Boundary element regularisation methods for solving the Cauchy problem in linear elasticity. *Inverse Problems in Engineering and Science*. 2002; 10 (4): 335-357.
 22. Marin, L., L. Elliott, D.B. Ingham and D. Lesnic. 2004. Parameter identification in isotropic linear elasticity using the boundary element method, *Engineering Analysis with Boundary Elements* 28(3), 221-233.
 23. Marin, L. and D. Lesnic. 2004. The method of fundamental solutions for the Cauchy problem in two-dimensional linear elasticity, *International Journal of Solids and Structures*, 41(13), 3425-3438.
 24. Marin, L. and D. Lesnic.. The method of fundamental solutions for inverse boundary value problems associated with the two-dimensional biharmonic equation. *Mathematical and Computer Modelling*, 2005; 42(3-4): 261-278.
 25. Galybin, A.N. A Method for determination of stress distributions in the process zone ahead of a 2D crack. In: Sarler B., Brebia C.A., editors. *Moving Boundaries VI*. Southampton: WIT Press. 2001. p. 243-252.
 26. Galybin, A.N. Determination of softening law by measuring crack opening displacements. In: Dyskin, A.V. Hu, X and Sahouryeh, E. editors, *Structural Integrity and Fracture*. Swets and Zeitlinger B.V., Lisse, The Netherlands, 2002. p. 35-41.
 27. Savruk, M. P. *Two-Dimensional Problems of Elasticity for Body with Cracks*, Naukova Dumka, Kiev, 1981.
 28. Leonov M.Y. and V.V. Panasyuk. Development of a nanocrack in a solid, In: Cherepanov G.P., editor. *Fracture: a topical encyclopedia of current knowledge*. Malabar, Florida: Krieger Publ. Com., 1998 (translated from *Prikladnaya Mekhanika*, 1959; 5(4): 391-401).
 29. Elices M., Guinea, G.V. Gomez J. and Planas, J. The cohesive zone model: advantages, limitations and challenges. *Engineering Fracture Mechanics*. 2002; 69 (2): 137-163.
 30. Que N.S. and Tin-Loi. F. Using WST results for the identification of the fracture parameters for the cohesive crack model. In: Valiappan S., Khalili N., editors. *Computational mechanics – New Frontiers for New Milenium*. Elsevier Science Ltd, 2001. p. 1109-1114.
 31. Bazant, Z. Concrete fracture models: testing and practice. *Engineering Fracture Mechanics*., 2002; 69 (2): 165-205.

Figures

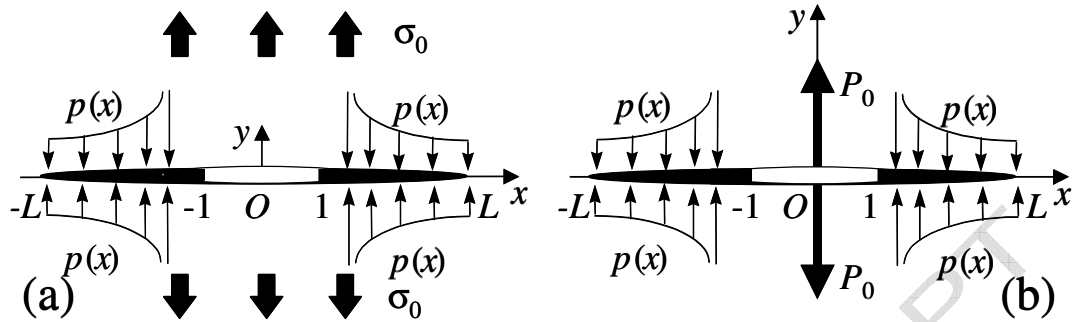


Figure 1 Cracks with process zones

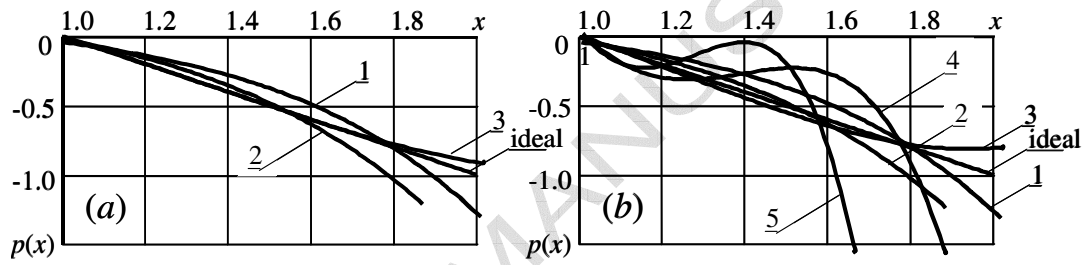
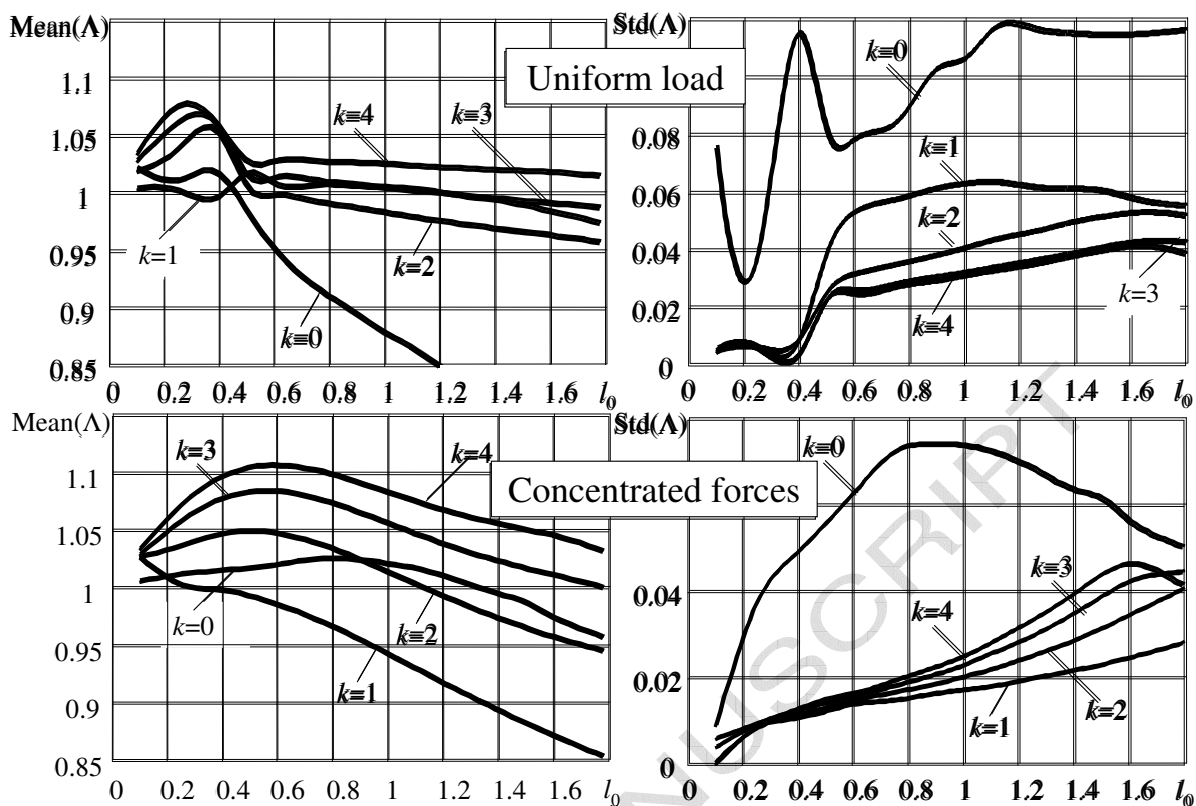
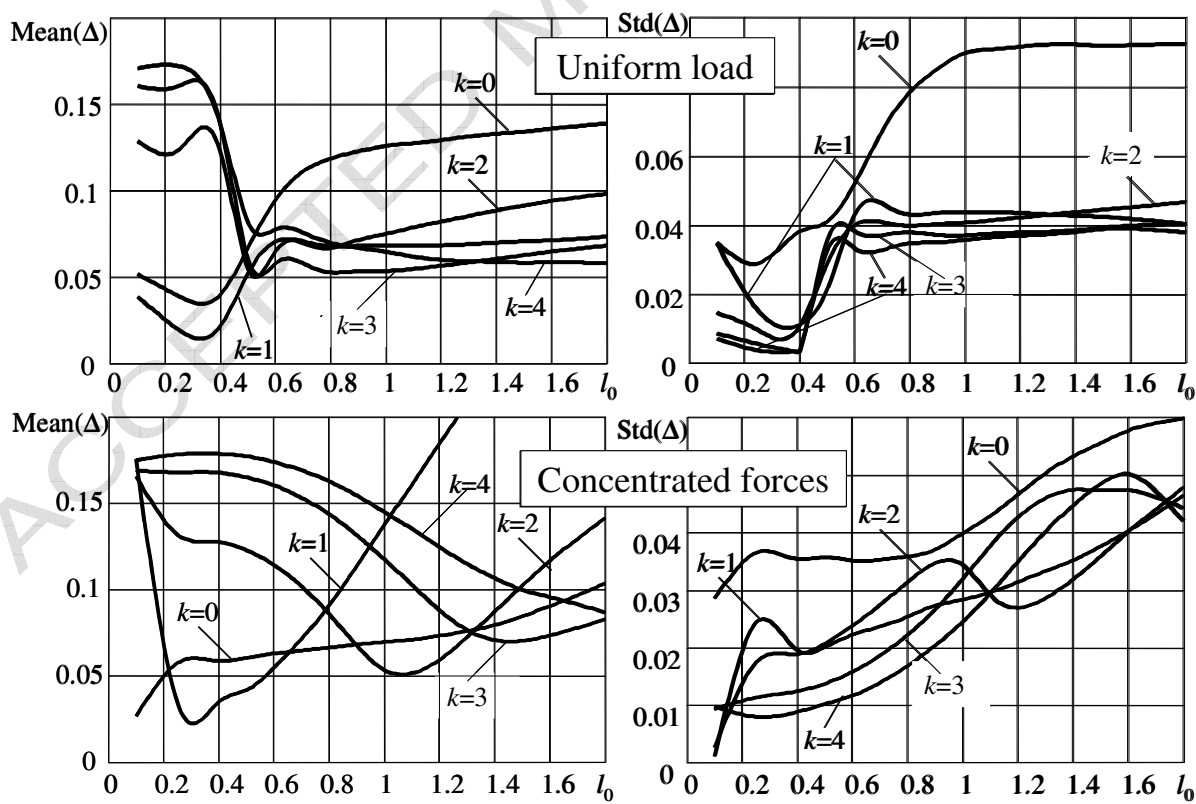


Figure 2 Deviation from the ideal linear stress distribution in the process zone for uniform loading of intensity $\sigma_0=0.436$: (a) – no distortion in the right hand side, (b) – 10% error. Digits refer to the number of non-zero diagonal elements in matrix D' .

Figure 3 Statistical characteristics of Λ .Figure 4 Statistical characteristics of Δ .

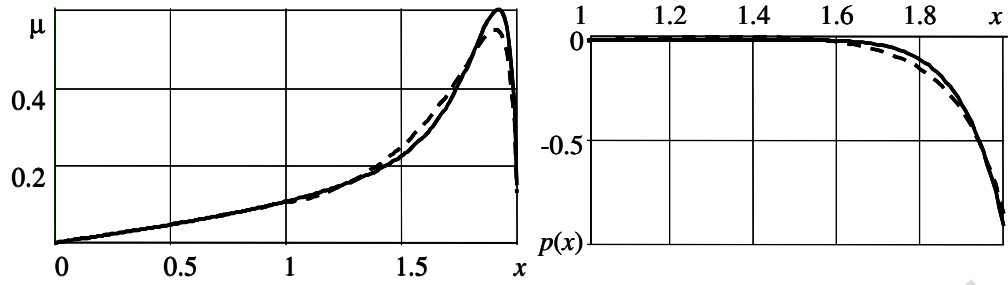


Figure 5 Examples of reconstructions obtained for the case of $L_0=2$ and $j=10$ with the normally distributed errors in the right hand side. Solid lines represent exact solutions; dashed line represents solution approximated by a polynomial of the 15th order, recovered parameter $L=2.00$.

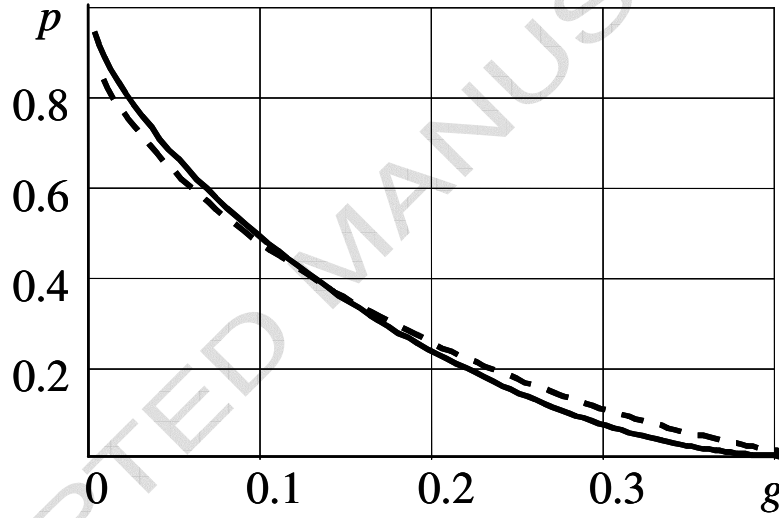


Figure 6 Ideal and recovered softening laws in the process zone of the crack in the plane subjected to uniform load at infinity for $L_0=2$ and $j=3$.

Table 1. Magnitudes of the loads used in modelling.

Load	$j=0$	$j=1$	$j=2$	$j=3$	$j=4$
$\sigma_0^{(j)}$	0.738	0.480	0.381	0.324	0.287
$P_0^{(j)}$	4.189	2.739	2.174	1.855	1.645